Journal of the Southeastern Association for Research in Astronomy, **6**, 41-46, 2012 July 10

NEW TRANSIENTS AS DETECTED BY THE FERMI GAMMA-RAY BURST MONITOR, JANUARY-JUNE 2011

Rebecca A. Robinson[1]
Department of Physics and Astronomy, Michigan State University, East Lansing, Michigan, 48825

and

Mark Leising
Department of Physics and Astronomy, Clemson University , Clemson SC 29634

ABSTRACT

After analyzing data collected by the Fermi Gamma Ray Space Telescope Gamma-Ray Burst Monitor (GBM), operated by NASA in cooperation with the US Department of Energy, we focus on transient gamma ray events from January of 2011. A number of these events were detected in concordance with events that have already been reported, and the others are analyzed in this report. For each event detected with a trigger-search computer algorithm, an energy spectrum was generated and these spectra were divided into several categories for further analysis. In some cases, intriguing spectral lines, including a 511 keV line, were detected; implications and analysis of these known and previously unknown events are discussed.

Subject headings: GRBs, Fermi, HXR, SXR, plasma astrophysics, magnetohydrodynamics, gamma rays: galaxies, gamma rays: stars

1. INTRODUCTION

1.1. *Background*

Like many great discoveries, transient gamma radiation from space was discovered by accident and as a result of international distrust and war. In 1963, the Nuclear Test Ban Treaty was signed, prohibiting the detonation of nuclear bombs in space. To verify compliance with the treaty, the United States launched the Vela satellites to patrol the skies; however when gamma-rays were detected, they were found to be not from terrestrial origin but rather from deep space. Since then, we have detected gamma- and X-ray emissions from some of the most cataclysmic and energetic events that have yet been discovered in the universe.

In the present day, the Fermi mission's Gamma-Ray Burst Monitor (GBM) views much of the sky from a low-Earth orbit in order to monitor supernova remnants such as the Crab nebula, quantify the high-energy effects of solar flares and coronal mass ejections from our own Sun, and detect gamma-ray bursts and transients (Meegan et al. 2009). The spacecraft contains fourteen detectors: 12 NaI detectors and 2 bismuth germinate (BGO) detectors. Using data collected from Fermi's GBM NaI detectors specifically, we search for statistically significant peaks in count rates and attempt to identify and locate the source of the high-energy photons detected. From January to June 2011, several potentially interesting events were observed and compared to known events in order to decide whether or not they may be significant gamma ray events. Primary results of this comparison study are discussed.

1.2. *Trigger-Search Algorithm*

The computer algorithm used to generate X- and gamma-ray spectra uses a web-based search program to gather data from the Fermi spacecraft, subtract background radiation based on measurements from two days prior to the given day as well as two days after, and plot transient events as counts versus time, for each detector. Each of the NaI detectors as well as the BGO detectors can be shown in one window to determine the validity of a detection, as events that trigger every detector are more than likely to be non-events. A second window contains a map of the Earth which indicates where the satellite was located in its orbit at the time of each detection. The Fermi spacecraft is turned off over the South Atlantic Anomaly (SAA) in order to prevent damage from the intense particle fluxes (Lemoine & Capdeville 2006), and its subsequent location with respect to the SAA is taken into account when analyzing data.

We choose a time in correlation with a possible event (new detections are denoted by a yellow line as shown in Figure 1) and, using the program's 'locate' function, we are able to generate a particle flux-based topographical sky map which indicates the most likely location of the source. In the case of a solar flare, the source will most likely be centered on a location marked with an 'S' on the map, as demonstrated in Figure 2 and will be noted with an 'F' in the original detector window as shown in Figure 1. The program imports information from the Fermi GBM Flare List in order to plot them on the detector window (`http://hesperia.gsfc.nasa.gov/fermi/gbm/qlook/fermi_gbm_flare_list.txt`). To notate a recorded transient gamma-ray event, a turquoise line appears on the detector window as well (Figure 1). In a final window, the spectrum of the event is generated as flux versus energy in kilo-electron volts. The overall shape of the spectrum as well as each potential spectral line event are both used to determine the nature of the event.

[1] Southeastern Association for Research in Astronomy (SARA) NSF-REU Summer Intern

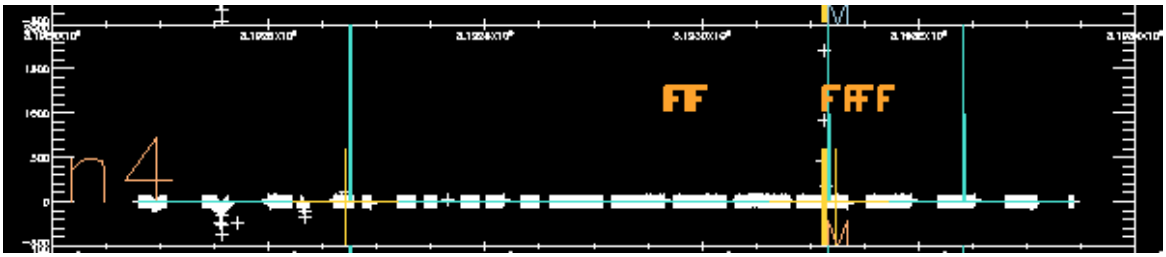

FIG. 1.— Example of a solar flare detection. February 13, 2011

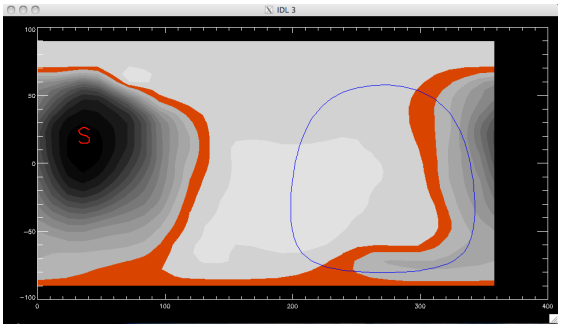

FIG. 2.— Example of a sky-map with contours representing goodness of fit (black is best fit) for a source in a given direction. This one is consistent with the direction to the sun (red S). April 30, 2011

2. PROCEDURE

2.1. *Sorting Triggers*

Between 2011 January to 2011 June, there were 19 known transient events detected by Fermi that have been identified as GRBs; all were in agreement with the documented time stamp within four percent. Five GRB events were detected in January, two in February, three in March, six in April, two in May, and one in June. It should be noted that these events were surrounded by many others, namely solar flares, land local particle events; however, the events discussed in this report are based on data collected from known GRB events.

Each of the spectra was sorted into four different categories based on shape and defining features: bulge, which has higher energy rates in the soft region of the spectrum; flare-like, which resembles the spectrum of a solar flare (Figure 3, top right); defined, which has obvious peaks at roughly 22 keV, 35 keV, 75 keV, 200 keV, and 511 keV; and noisy, which has no specific pattern and can only be described as chaotic or sporadic. An example of each category is given in Figure 3. Using these categories as bases for comparison, we combed through the Fermi GBM data once again to find events that resembled the known events but had not been reported as of yet.

For the initial rough search, several characteristics of the detections were explored. The number of detectors that detected the event as well as the proximity to the SAA were both taken into account, in addition to the ability of the program to define (or not define) an approximate location for the event, based on the relative rates in the various detectors. This ability to pin down some sort of location was given a considerable amount of influence during the initial search for events, because an event that could not give a general direction, for example, local particles interacting nearly equally in all detectors, is not likely a celestial photon event. However, after the initial search, much more weight was placed on the spectra. Candidates were sorted into the same four spectral categories as the known events.

For the purpose of qualitatively examining the characteristics of the detections, each event was then sorted into a category that described the caliber of the results. To elaborate, each event was placed into a group of detections with either well-defined detector read-outs, well-defined topographical directional maps, neither of those, or both. This allowed me to organize event quality in a very simple manner.

Next, each of the four categories were sorted into two subcategories based on proximity to the SAA, since events have been detected both far away from the SAA and properly on the edge of the SAA. This is illustrated in Figure 4.

Then, the detectors were examined in order to determine whether the spectrum seemed to be GRB-like or some 'other' form of event, which is shown in Figures 5 and 6. This was determined simply by looking at the detectors from the known events and noting the shapes and patterns of the spectra.

Using this, the GRB-like events were sorted into two categories: sudden, which means that durations were very short, having a burst-like quality; and Gaussian, which describes a bell-curve shape (Figure 5). The 'other' events were also sorted into two categories: rising, which describes rates that rise steadily, often at the edge of the SAA; and random (Figure 6). Note that the vast majority of GRB candidates were classified as GRB-like and 'sudden'. A similar sorting algorithm was applied to the known events in order to get an idea of how well these new events could compare, and then flow charts were generated to organize the numerous characteristics of both the known events and the new events (Figures 7 and 8).

For the purpose of narrowing down the events further, I isolated the branches of each flow-chart (Figures 7 and 8) that matched exactly, as illustrated in Figures 9 and 10. The matching branches were then analyzed further, under the assumption that these events were more likely to describe an actual GRB event. Analysis of these events is discussed in Section 3 below. Special attention is paid to the 'Defined', 'Bulge', and 'Flare-like' spectral categories for the purposes of this report.

3. RESULTS AND DISCUSSION

3.1. *Evidence for GRBs*

Since Fermi's GBM has detected GRBs before, the simplest way to search for more GRB events is to empirically compare characteristics of known GRB events to candidates. By this logic, the matching branches of the GRB flow-charts (Figures 9 and 10) are the most-likely candidates for newly discovered GRBs. In these cases, we

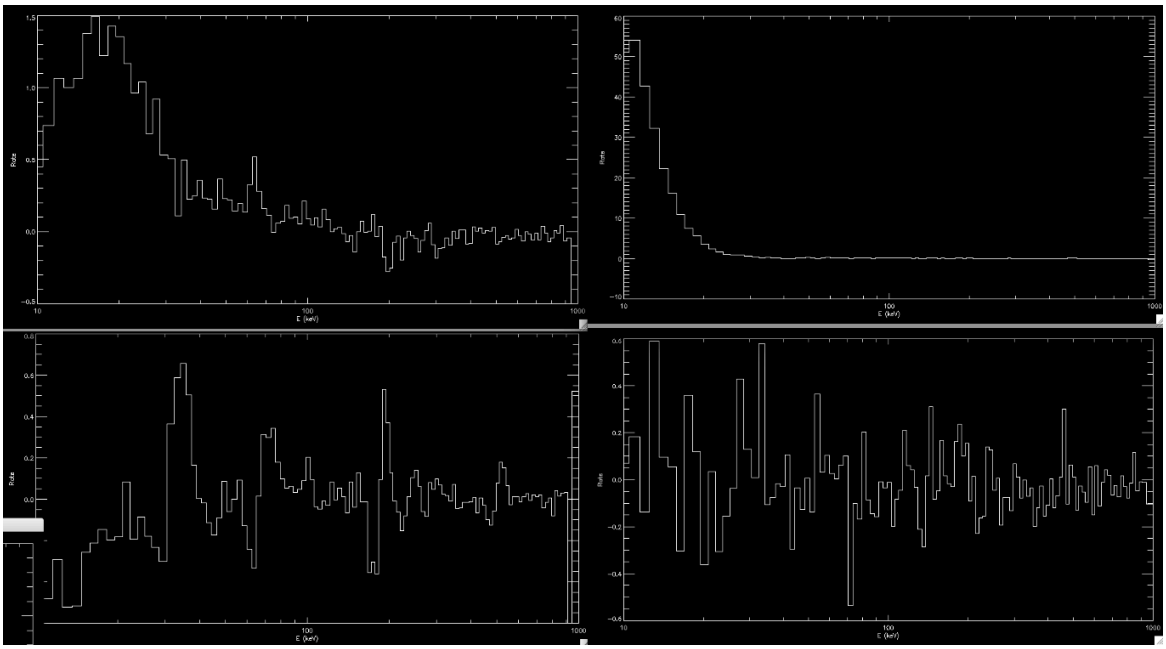

FIG. 3.— Bulge (top left), Flare-Like (top right), Defined (bottom left) and Noisy (bottom right)

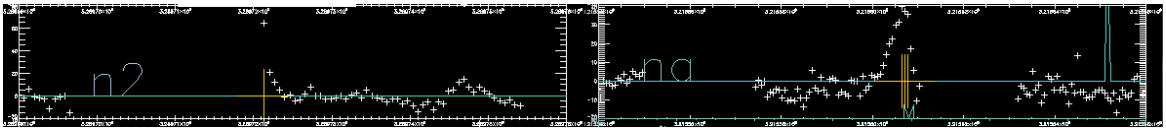

FIG. 4.— Detection on the edge of the SAA (left) versus a detection farther away from the SAA

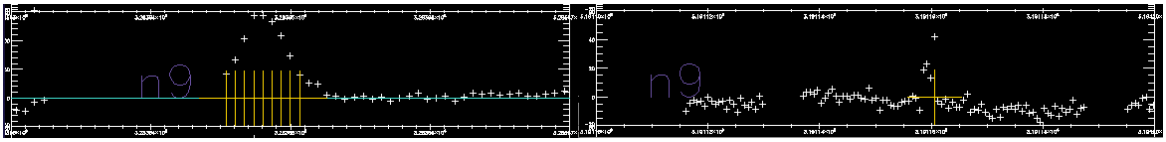

FIG. 5.— Examples of GRB-like events, both sudden (left) and Gaussian (right)

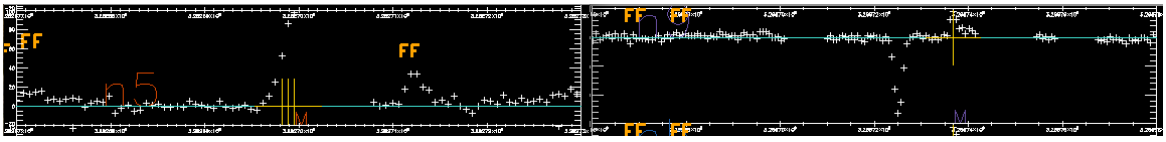

FIG. 6.— Examples of events that are not GRB-Like, or 'other'; rising (left) and random (right)

have discovered events corresponding to all four spectral categories, events that were detected both near and far from the SAA, and events that appear to be burst-like, sporadic, and symmetric. The range of newly detected events is nearly as wide as the range of known events, which suggests that every GRB is different and specific to its own source and context. By analyzing these events, we have found that a wide variety of peak energies, peak count rates, time spans, and spectral lines exist in our sample. Possible explanations of these interesting trends are discussed in the following sections.

3.2. *Explanation of Defined Spectra*

Spectra assigned to the category "Defined" were placed there because of prominent lines at roughly 22 keV, 35 keV, 75 keV, 200 keV, and 511 keV. (It should be noted that each of these energies below 100 keV may be correct within a margin of error of roughly ±5 keV, and those above 100 keV may be correct within a margin of error of ±50 keV.) It is well known that the 511 keV line represents the electron-positron annihilation line, which can result from many different events in a plasma state. However, the other lines are less well-defined. One possible explanation for these spectral lines is that the excitation may not be extra-terrestrial in nature, but rather may have been a result of the excitation of isotopes on the detectors on board. There are two different types of detectors: NaI and BGO. Due to bombardment by cosmic rays or other high-energy particles, isotopes of either sodium, iodine, bismuth, or germanium may have been heightened to excited energy states and then decayed shortly after. For example, the 35 keV and 200

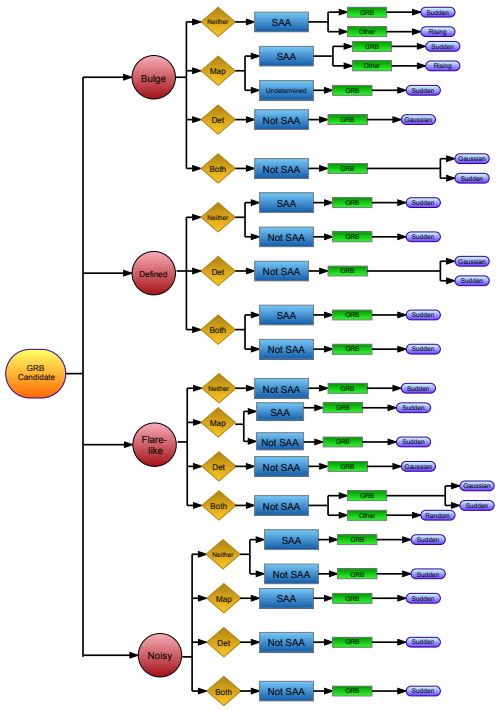

FIG. 7.— Flow chart describing the organization of GRB candidate events

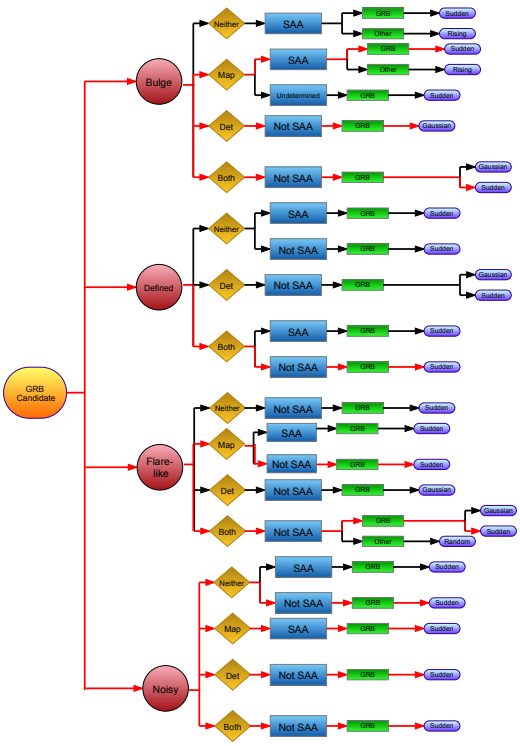

FIG. 9.— Flow chart describing the organization of GRB candidate events with isolated matching lines (shown in red)

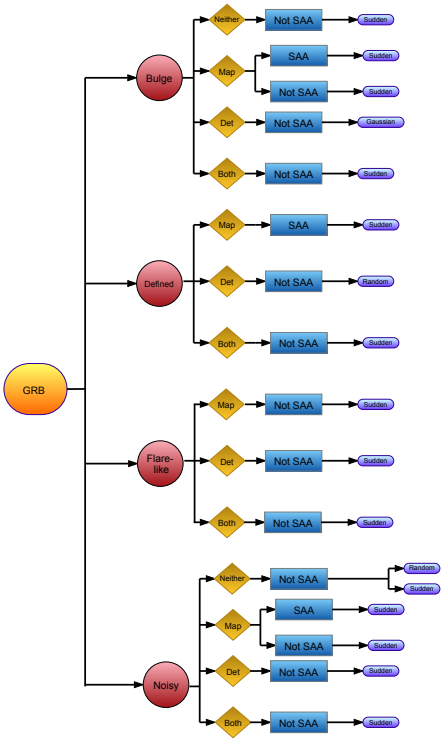

FIG. 8.— Flow chart describing the organization of known GRB events

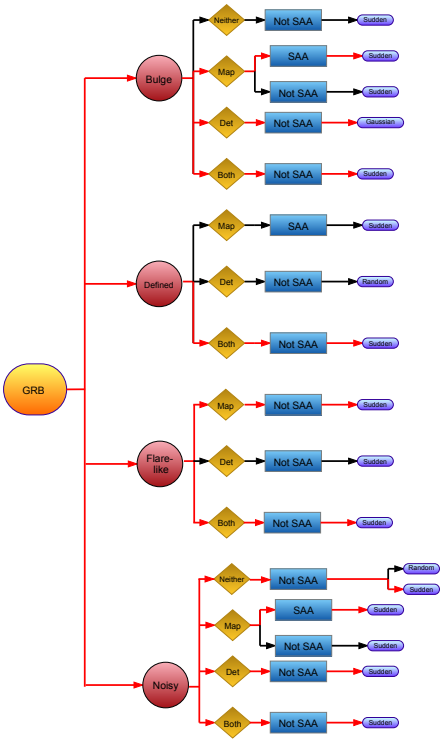

FIG. 10.— Flow chart describing the organization of known GRB events with isolated matching lines (shown in red)

keV lines may be described by IT decay of meta states of Iodine-130 and Germanium-71, having decay energies of 40 keV and 198 keV, respectively. A second possible explanation for the 200 keV line could be the electron capture of Germanium-71 to Gallium-71, having an energy of 229 keV (Firestone et al. 1999). In addition, the 75 keV line corresponds heavily with the k-α X-ray energy of Bismuth-209 However, these are merely possible explanations and have not been confirmed. As for the 22 keV line, this remains largely a mystery. The energy corresponds most heavily with k-α X-ray energies of silver and cadmium, but there is little evidence of the existence of these elements in this scenario. There is no reason to believe the lines we do see come from other than particle irradiation of the instrument.

3.3. *Discussion of Bulge Spectra*

An interesting trend was noticed from the spectra within the 'Bulge' category. As illustrated in Tables 1 and 2, only events that fall into this category have any chance of lasting longer than a short, instantaneous burst. That is not to say, however, that every Bulge spectrum has a time-span, but rather the only spectra with time-spans are Bulge spectra. These excitations last anywhere from roughly half of a minute to roughly twelve minutes. Looking at the detectors for these events, many of them fall under the 'Gaussian' category and have incredibly striking symmetry. Based on the spectra, these events could certainly be described as long-soft GRB events (as discussed in Section 1.2) because the bulges occur at lower energies. In addition, many of these events are only detected on half of the detectors, which is interesting because half of the detectors face one direction and the other half of the detectors face an opposite direction. This implies that the sources of many of these longer-lived detections come from a specific direction, which is certainly helpful information. As noted in Tables 1 and 2, all of these events seem to peak between 15 keV and 30 keV; however the count rates at those peaks range from 0.95 to 8.25 ct/s/keV. Clearly, some of the events are more luminous than others, but they are still incredibly soft in the energy scale. Since the majority of the spectra indicate this softer energy range (<100 keV), it is also possible that these may be thermal in nature.

3.4. *Other Possibilities*

None of the events detected were plotted in direct concordance with an 'F', denoting a solar flare; nor do the majority of them appear to be in the direction of the sun. However, just because the events do not coincide with a flare does not necessarily mean that they are not solar in nature. Additionally, it was found that spectra with the two greatest count rates (both with known GRBs and with GRB candidates) were 'Flare-like' spectra (Tables 1 and 2). Although these events are not on record as being solar flares and do not necessarily point towards the sun, such a large count rate cannot be ignored. It is possible that these particularly luminous events could actually be a result of solar activity. Atmospheric scattering is not taken into account in our directional determinations.

In the same way, we would be remiss in my report if we did not explore the possibility that many of these GRB candidates may in fact be local particles. Many of them occur at the edge of the SAA, meaning that there exists a possibility that these triggers could simply be local particles, specifically electron precipitation. As Earth's magnetic field is pushed by the solar wind, trapped electrons can be released and spiral down the field lines into Earth's atmosphere(Goedbloed & Poedts 2004). This could explain a sudden burst near the SAA. However, many of the known GRB events occurred when the detectors were on the proper edge of the SAA. Therefore, it is difficult to determine whether or not candidates were excited due to particle precipitation. Of course, this does raise the possibility that, perhaps, some of the events that identify as GRBs are actually, in fact, particle precipitation. This easy mistake is not unheard of; for example, GRB event 110316205 was initially assigned GRB status until it was confirmed that the event was actually triggered by local particles near the SAA. However, for the time being, we can only assume that the known GRB events are actual GRB events, and the candidates that resemble GRB events are also just that.

4. CONCLUSION

Of the 19 known GRB events detected between January and June of 2011, characteristics of 11 of these events directly match with characteristics of 29 potential GRB candidates (Tables 1 and 2). Matches were based on spectral shape, success of the trigger-search algorithm results, proximity of the detection to the South Atlantic Anomaly (SAA), and detection type. Other possible explanations for the events include local particle precipitation. To continue, the next step would be to analyze the BGO detectors for each candidate, as this report did not focus on those detectors.

The author wishes to acknowledge NASA's Fermi Gamma-ray Space Telescope mission and all persons affiliated with the SARA REU Program of 2011, as well as the National Science Foundation for providing funding for this project through the Research Experiences for Undergraduates (REU) program, grant NSF AST-1004872.

REFERENCES

Firestone, R. B., Ekstrom, L. P., & Chu, S. Y. F. 1999, APS Division of Nuclear Physics Meeting Abstracts, 13

Goedbloed, J. P. H., & Poedts, S. 2004, Principles of Magnetohydrodynamics, by J.P.H. Goedbloed and S. Poedts. UK: Cambridge University Press, 2004.,

Lemoine, J.-M., & Capdeville, H. 2006, Journal of Geodesy, 80, 507.

Meegan, C., Lichti, G., Bhat, P. N., et al. 2009, ApJ, 702, 791

Tajima, T., & Shibata, K. 2002, Plasma astrophysics /T. Tajima and K. Shibata. Cambridge, Mass. : Perseus, 2002. / (Frontiers in physics ; v.98)

TABLE 1
Known GRB Events

GRB Date	$E_{\rm peak}$ (keV)	$\rm Rate_{peak}$ (ct/s)	Detector	$t_{\rm start}$	$t_{\rm end}$	Δt (s)	Spectral Category
110102	30	1.8	n0,n1,n2,n4,n6,n8,n9,na	18:54:56	18:55:28	32	Bulge
110118	35	0.65	n9	20:33:36	20:33:36	0	Defined
110123	25	0.9	n0,n1,n3,n4,n5,n6	19:17:20	19:17:20	0	Bulge
110213	15	1.25	n3,n4,n5,n8	05:16:48	05:16:48	0	Noisy
110301	10	24.5	n3,n4,n6,n7,n8,n9,na,nb	05:08:16	05:08:16	0	Flare−Like
110304	65	0.45	n5	01:41:52	01:41:52	0	Noisy
110322	15	0.59	n3	13:23:12	13:23:12	0	Noisy
110428	35	0.3	n0,n3,n4,n5,n6,n7,n8	09:17:52	09:17:52	0	Noisy
110430	12	54	n6,n7,n9	09:00:16	09:00:16	0	Flare−Like
110517	20	1.15	n6,n7,n8,nb	13:44:32	13:44:32	0	Noisy
110609	30	0.95	n1,n2,n4,n5,n7	04:30:56	04:40:00	544	Bulge

Note. — This table describes the known GRB events as detected by the Fermi Gamma-Ray Space Telescope (GBM). The date is shown (YYMMDD), followed by the peak energy and count rate, then the detectors that were excited by the event. The 'n' represents the NaI detectors. Then, the starting and ending time are given for each event, as well as a time span if applicable. Finally, the spectral category is given. Note that all times are given in UT.

TABLE 2
Candidate GRB Events

GRB Date	$E_{\rm peak}$ (keV)	$\rm Rate_{peak}$ (ct/s)	Detector	$t_{\rm start}$	$t_{\rm end}$	Δt (s)	Spectral Category
110112	12	12	n0,n2,n4,n5,n6,n7,n8,n9,na,nb	11:22:08	11:22:08	0	Flare−Like
110118	12	0.59	nb	13:52:32	13:52:32	0	Noisy
110206	15	3.6	n3,n9	13:33:52	13:33:52	0	Flare−Like
110209	15	0.9	n9	11:29:36	11:29:36	0	Defined
110211	20	3.6	n9,na,nb	11:21:04	11:21:04	0	Bulge
110221	20	0.6	n5,n6,n7	03:40:48	03:40:48	0	Noisy
110221	20	0.5	na	12:20:16	12:20:16	0	Noisy
110224	20	1.0	nb	01:41:52	01:41:52	0	Bulge
110224	15	3.3	nb	04:48:00	04:48:00	0	Flare−Like
110225	12	2.05	n6,n7,n9	22:40:32	22:40:32	0	Flare−Like
110305	20	0.45	n9,na	12:25:36	12:25:36	0	Noisy
110311	20	1.15	n4,na	18:24:00	18:26:08	128	Bulge
110314	12	72.5	n5	00:17:04	00:17:04	0	Flare−Like
110316	35	0.5	n9,na	18:02:08	18:02:08	0	Defined
110401	15	0.725	n2,nb	09:26:24	09:26:24	0	Noisy
110404	13	0.475	n4,n6,n7,n8,n9,na,nb	04:21:20	04:21:20	0	Noisy
110406	25	0.675	n9,na	07:18:56	07:18:56	0	Defined
110407	22	0.5	n6,n7,n8,na	05:37:36	05:37:36	0	Noisy
110409	15	1.8	n0,n1,n3,n4,n5,n6,n7,n9,na,nb	17:40:16	17:41:52	96	Bulge
110512	15	7.25	n1,n5,n9,na	20:50:08	20:50:08	0	Flare-Like
110514	35	0.8	All	20:25:04	20:25:04	0	Noisy
110526	35	0.5	n6,n7,n9	05:09:20	05:09:20	0	Noisy
110527	15	1.65	All	00:19:12	00:19:12	0	Bulge
110529	20	3.7	n0,n1,n2,n6,n9,,na,nb	12:25:36	12:30:56	320	Bulge
110605	20	8.25	n6,n7,n8,n9,na,nb	03:22:08	03:30:08	480	Bulge
110608	20	6.25	n6,n7,n8,n9,na,nb	04:37:52	04:49:36	704	Bulge
110609	20	5.5	n6,n7,n8,n9,na,nb	02:53:52	03:01:52	480	Bulge
110611	30	4.6	n6,n7,n8,n9,na,nb	05:51:28	05:58:24	416	Bulge
110623	15	2.1	n4,n6,n7,n8,n9,na,nb	03:52:00	03:53:04	64	Bulge

Note. — This table describes the candidate GRB events as detected by the Fermi Gamma-Ray Space Telescope (GBM). The date is shown (YYMMDD), followed by the peak energy and count rate, then the detectors that were excited by the event. The 'n' represents the NaI detectors. Then, the starting and ending time are given for each event, as well as a time span if applicable. Finally, the spectral category is given. Note that all times are given in UT.